Journal of the Serbian Chemical Society

ANN prediction of the efficiency of the decolourisation of organic dyes in wastewater by plasma needle

TATJANA Đ. MITROVIĆ[1]*, MIRJANA Đ. RISTIĆ[2#], ALEKSANDRA PERIĆ-GRUJIĆ[2#] and SAŠA LAZOVIĆ[3]

[1]*Institute for Water Resources "Jaroslav Černi", Belgrade, Jaroslava Černog 11226, Belgrade, Serbia, [2]University of Belgrade, Faculty of Technology and Metallurgy, Karnegijeva 4, 11000 Belgrade, Serbia and [3]Institute of Physics Belgrade, University of Belgrade, Pregrevica 118, 11080, Zemun-Belgrade, Serbia*

Abstract: In this paper, the results of decolourisation of Reactive Orange 16 (RO 16), Reactive Blue 19 (RB 19) and Direct Red 28 (DR 28) textile dyes in aqueous solution by plasma needle are presented. Treatment time, feed gas flow rate (1, 4 and 8 dm^3 min^{-1}) and gas composition (Ar, Ar/O_2) were optimized to achieve the best performance of the plasma treatment. An artificial neural network (ANN) was used for the prediction of parameters relevant for the decolourisation outcome. It was found that more than 95 % decolourisation could be achieved for all three dyes after plasma treatment, although the decolourisation of DR 28 was much slower than those of the other two dyes, which could be explained by the complexity of its molecular structure. It was concluded that the oxidation was very dependent on all three mentioned parameters. The ANN predicted the treatment time as the crucial factor for decolourisation performance of RO 16 and DR 28, while the Ar flow rate was the most relevant for RB 19 decolourisation. The obtained results suggest that the plasma needle is a promising tool for the oxidation of organic pollutants and that an ANN could be used for optimization of the treatment parameters to achieve high removal rates.

Keywords: textile dyes; oxidation; plasma discharge.

INTRODUCTION

The hazardous effects of increasing industrialization and agriculture affect the water ecosystem and human health directly. Considering the amounts of various industrial wastewaters discharged into different water bodies, the activities in the water purification research area are influenced. Due to their operations, the textile, food and paper industries generate very complex and diverse

effluents and they are rated as one of the most polluting among all industrial sectors.[1] The main components of these effluents are organic dyes (colorants), noted in the literature as very toxic, mutagenic and carcinogenic.[2–4] About 700 000 t of textile dyes produced annually are discharged into different water bodies disturbing their quality directly (colour, chemical oxygen demand (*COD*), biological oxygen demand (*BOD*), suspended solids, temperature, pH, dissolved O_2, *etc*.).[5]

Among all categories widely used in industry, there are azo and anthraquinonic types of dyes. Since they are made to be very chemically resistant and stable, mineralization by bacterial activity is very low and the water purification treatment very demanding.[6] Some of the traditional techniques, such as biological treatment,[7] adsorption,[8] nanofiltration[9] and ozonation[10] are being already used but with some limitations.[6] The biggest problem concerning all the mentioned processes is the formation of secondary pollution with no complete degradation of the final disposal.[11,12]

Hence, very strict international environmental standards must be accomplished. In order to achieve these restrictions (ISO 14001, Directive 2000/60/EC of the European Parliament – WFD), many conventional technologies have been used for effective decolourisation and degradation of various pollutants as has seen, but due to their inefficiency, operational and economical expenses, other alternative approaches had to be studied.

During the last few decades, advanced oxidation processes (AOPs) have attracted large attention for water purification treatment[13] as very suitable for the degradation of colorants that are resistant to the above-mentioned common technologies.[14] They are used successfully in the mineralization of soluble complex organic pollutants up to CO_2, H_2O and inorganic ions without any additional waste treatment and disposal.[15] Compared to common chemical oxidizing processes, such as chlorination and ozonation, they do not produce any toxic by-products.[16]

Among all AOPs (UV/H_2O_2, UV/ultrasound, photo-Fenton, heterogeneous photocatalysis, UV/TiO_2, *etc*.) plasma processes have also been investigated as a novel method for wastewater decontamination.[17,18] There are various types of non-thermal plasma devices, such as plasma jets, plasma needle, gliding arc, *etc*.[19] These methods have a strong oxidizing ability and include simple operating conditions, such as temperature and atmospheric pressure. Producing electron, radicals (hydroxyl radical, hydrogen radical, hydroperoxyl radicals), ions (OH⁻, H_2O^+, H⁺, HO_2^-) and neutrals (H_2O_2, O_3) with very high reduction potentials, powerful UV radiation and shock waves, the plasma decomposes organic matter with no additional procedures and no sludge production.[20] These characteristics make it convenient for different applications: sterilization, decontamination, purification, *etc*.

Plasma oxidation processes in liquids have been widely examined. Through the plasma treatment, various complex chemical reactions are initiated in the solution that is being treated. It is concluded that oxidation mechanisms occur because of the formation of reactive radicals, which strongly depend on the quality and quantity of the feed gas and the properties of the treated sample.[21]

ANN is a powerful technique for modelling nonlinear multivariable systems, where the variables may have complex interrelationships that cannot be easily defined, such as in plasma oxidation processes.[20] Concerning the complexity of the oxidation mechanism initiated by AOPs, the modelling of the removal process using artificial neural network (ANN) techniques was previously investigated[22] as it does not require a mathematical description of the observed process. In the current study, ANNs were applied for the prediction of decolourisation efficiency of organic dyes by plasma discharge treatment on changing the process conditions.

The main goal of this work was to estimate the efficiency of the plasma oxidation process on samples of various textile dyes by finding the best operational parameters (treatment time, flow rate and composition of the feed gas) and the possibility of prediction the effects oxidation based on ANN algorithms.

EXPERIMENTAL

All dyes were from Sigma–Aldrich (St. Louis, MO, USA) and used without any further purification. Their main characteristics are given in Table I, while their structural formulas are presented in Fig. 1.

TABLE I. Main characteristics of the model dyes used in plasma treatment

Commercial name	Bezactive Orange V-3R	Remazol Brilliant Blue R	Congo Red
Functional group	Azo	Anthraquinone	Azo
C. I. name	Reactive Orange 16 (RO 16)	Reactive Blue 19 (RB 19)	Direct Red 28 (DR 28)
Molecular weight g mol^{-1}	617.54	626.54	696.66
Wavelength (max), nm	493	592	497

Dye samples were prepared with distilled water ($c = 50$ mg L^{-1}, $V = 50$ mL). The plasma needle setup used in this research (Fig. 2) comprised of a Teflon body with a copper electrode placed in the glass cylinder. Detailed characterisation of this plasma source is presented elsewhere.[23] The needle tip was immersed in the solution. A magnetic stirrer (300 rpm) preserved the homogeneity of the sample. Different Ar flow rates (1, 4 and 8 dm^3 min^{-1}) were used with different percentages of added O$_2$ in the feed gas. The plasma oxidation effect was determined by measuring the decolourisation rate of the dyes. After all treatments, the samples were analysed using a UV/Vis spectrometer (Varian Superscan 3, USA) by measuring absorbance (A) at characteristic wavelengths (Table I).

The ANN architecture used in this study consisted of several layers of neurons, namely the input layer, the hidden layer(s) and the output layer (Fig. 3). The ANN works by introducing the values of the available inputs to the neurons of the first layer, where each input

MITROVIĆ *et al.*

value is multiplied by a coefficient (weight) and forwarded to the neurons in the hidden layer in which the weighted sum is computed. Finally, the results are then forwarded to the output layer and compared to the measured values in order to evaluate the model performance.
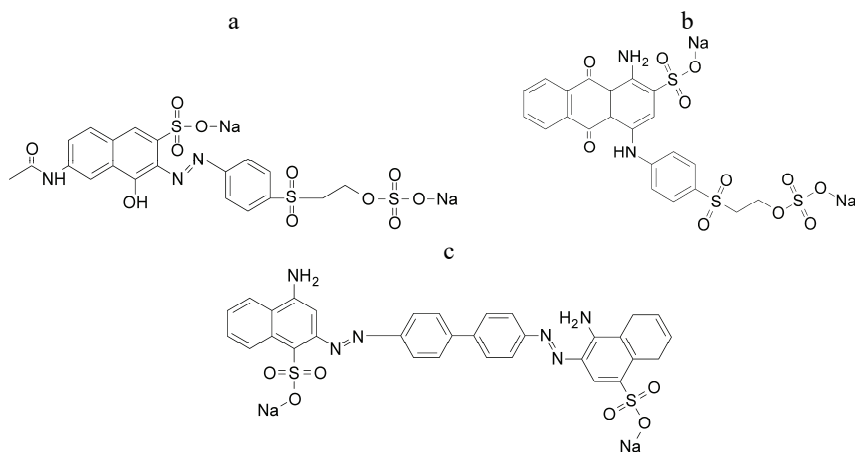

Fig. 1. Structural formulas of the textile dyes used in the plasma treatment: a) RO 16, b) RB 19 and c) DR 28.
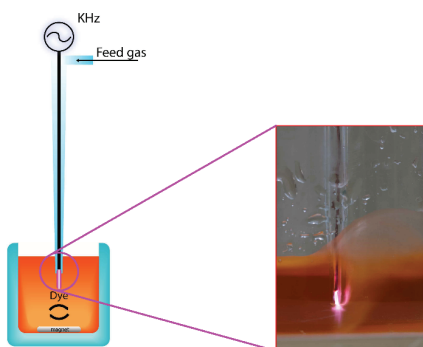

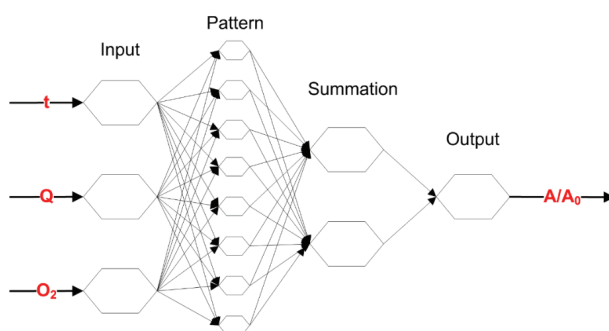Fig. 2. Plasma needle experimental setup.

Fig. 3. Graphic representation of the created ANN model.

Among various ANN algorithms, the general regression neural network (GRNN) demonstrated very good results in fitting complex systems with a limited set of training data.[24–26] In present work, this architecture was selected because of its ability to fit multidimensional datasets even with sparse data points. The GRNN structure is fully adjusted to the modelling system, namely the size of each of four layers (expressed as the number of neurons) depends only on the number of used input/output variables and data patterns in the dataset used for training.

The training process between the input layer and the hidden layer was composed of unsupervised learning, while the training between the hidden layer and the summation layer was composed of supervised learning, with the aim of minimizing the difference, *e.g.*, the mean square error, between the model output and target value.[27] More details on the GRNN algorithm can be found in relevant literature.[28]

RESULTS AND DISCUSSION

Plasma oxidation process

During the plasma treatment, many chemical reactions are introduced because of inelastic collisions of high-energy electrons arising from the interaction of the plasma with water molecules (Fig. 4).
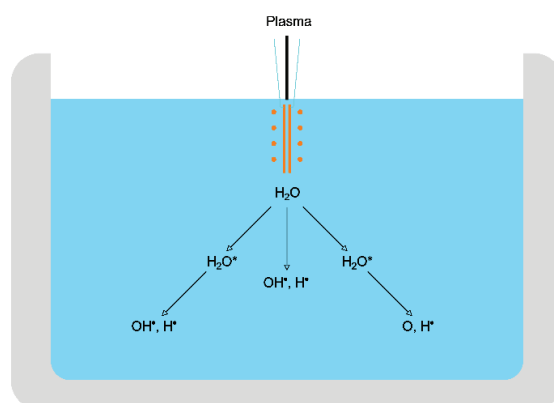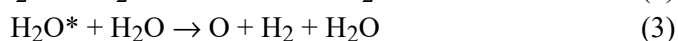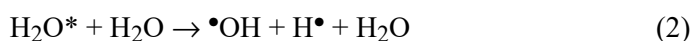

Fig. 4. Important chemical species in the liquid phase induced by the plasma needle.

According to the literature,[20] these collisions lead to the most significant processes, such as vibrational or rotational excitation of neutral water molecules (Eq. (1)):

$$H_2O + e^- \rightarrow H_2O^* + e^- \qquad (1)$$

After the electron excitation, water relaxes into a lower energetic state through any of following three reactions (Eqs. (2)–(4)):

$$H_2O^* + H_2O \rightarrow {}^\bullet OH + H^\bullet + H_2O \qquad (2)$$

$$H_2O^* + H_2O \rightarrow O + H_2 + H_2O \qquad (3)$$

$$H_2O^* + H_2O \rightarrow O + 2H^\bullet + H_2O \qquad (4)$$

If the electron energy is high enough to overcome the water dissociation threshold (>7 eV), then other reactions could occur, leading to the water molecule dissociation (Eq. (5)):

$$H_2O + e^- \rightarrow {}^{\bullet}OH + H^{\bullet} + e^- \qquad (5)$$
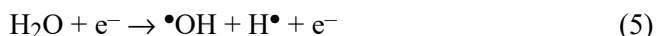
Production of radicals by plasma discharge in water has been examined by optical emission spectroscopy. It was reported that the key radical species in a plasma are the very powerful oxidizing species ${}^{\bullet}OH$ formed as a consequence of vibrational/rotational excitation of water (Eq. (2)) or directly by the electron impact dissociation of water (Eq. (5)).[20] Having a standard reduction potential of $E^0 = 2.85$ V, it could initiate decolourisation reactions by reacting with the dye molecules with a high reaction rate ($\approx 10^9$ L mol^{-1} s^{-1}).[29]

Chemical properties (possibility of oxidation, biodegradation) of the dyes are related to the chemical structure of each dye. Three textile dyes were chosen as representatives because of their different structures. RO 16 and DR 28 are categorized as azo dyes whereby RO 16 has one azo group (–N=N–) and DR 28 two as chromophores. RB 19 with the chromophore groups =C=O and =C=C= forming an anthraquinone complex was selected as a representative from the class of anthraquinones. All three dyes are characterized by high chemical stability and resistance to conventional physical and chemical degradation processes due to their complex, aromatic compositions.[29,30]

The oxidation rate of the dyes was determined following the colour loss (decolourisation) process. It was the evidence that the chromophore group that was responsible for the absorption of the dye molecule in the visible region of the spectral range had been eliminated. Decolourisation rates for all three colorants are presented in Figs. 5 and 6.

The most noticeable fact is that the decolourisation was faster at the beginning of the plasma treatment and slowed down as the treatment continued because of different affinity of the reactive species for the different parts of the dye molecule. The radicals initially attacked the chromophore group, causing simultaneously fast decolourisation. Subsequently, the benzene and naphthalene groups of the dye molecules were probably mineralized to lower molecular weight acids and CO_2,[31] amino groups to nitrate, azo groups to gaseous N_2 and sulphonates to sulphates.[32]

The absorbance decrease and almost total decolourisation achievement after a certain time of plasma treatment (depending on the dye) for all Ar flow rates (1, 4 and 8 dm^3 min^{-1}) are shown in Fig. 5. RO 16 and RB 19 have similar decolourisation trends, while DR 28 was found to be much more demanding for complete decolourisation. A faster decolourisation rate is evident as the Ar flow rate increases. Comparing the decolourisation kinetics for 1, 4 and 8 dm^3 min^{-1} during the first 30 min of treatment, the decolourisation rate significantly inc-

reases especially for the RO 16 and RB 19. However, after 30 min, the increase of flow rate did not contribute significantly to the decolourisation rate. Namely, after 15 min of RO 16 treatment, 80 % of dye had been decolourised (8 dm^3 min^{-1}), 60 % for 4 dm^3 min^{-1} and only 30 % for 1 dm^3 min^{-1}. RB 19 did not follow this pattern.
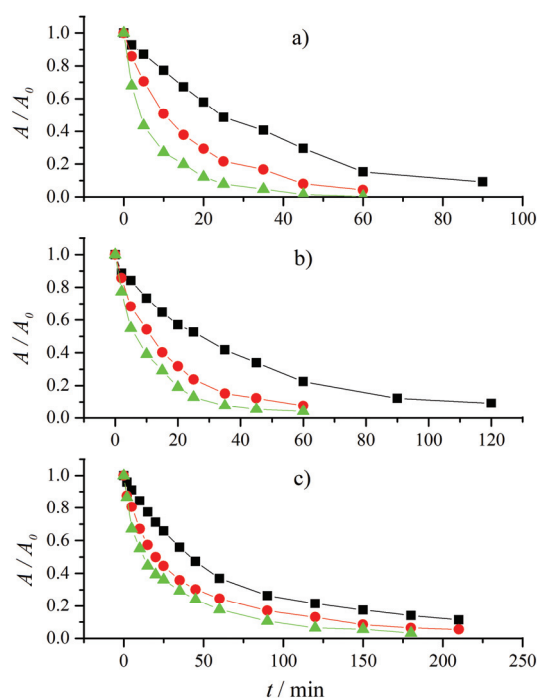

Fig. 5. Decolourisation rates of textile dyes: a) RO 16, b) RB 19 and c) DR 28 during plasma treatment for different Ar flow rates (-■- 1 dm^3 min^{-1}, -●- 4 dm^3 min^{-1}, -▲- 8 dm^3 min^{-1}).

The difference between 1 and 4 dm^3 min^{-1} is obvious indicating that the feed gas flow rate is crucial for the oxidation process, reducing the time for complete decolourisation from 120 to 60 min. Regarding DR 28, bearing in mind the complexity of its molecular structure, it was very demanding to achieve a satisfying decolourisation effect, but with prolonged treatment time the effect was realised. It is evident that the time for entire decolourisation was prolonged in comparison to that required for the two previous dyes and that the feed gas flow rate also did not have a satisfying influence on the oxidation effect, as for RO 16 and RB 19.

Accordingly, the decolourisation rates followed the order: RO 16 > RB 19 > DR 28. This order was caused by the diverse molecular structure of each dye. Anthraquinone dyes (RB 19) are more resistant to degradation due to their fused aromatic structures that are resonance stabilized compared to azo ones (RO 16).[33]

The results obtained in this research are in agreement with those of the studied literature, where the faster RO 16 decolourisation process with ozone oxidation compared to RB 19 is confirmed.[34] The smallest decolourisation rate of DR 28 could be explained by the large aromatic molecule with two conjugated azo groups (chromophores), which intensify the colour of the dye leading to the prolonged time of the oxidation process.

In the present work, when a certain percentage (2 or 5 %) of O_2 was added in the feed gas (Fig. 6) for the same flow rate (4 dm^3 min^{-1}), the decolourisation performance was significantly enhanced, especially for RB 19.
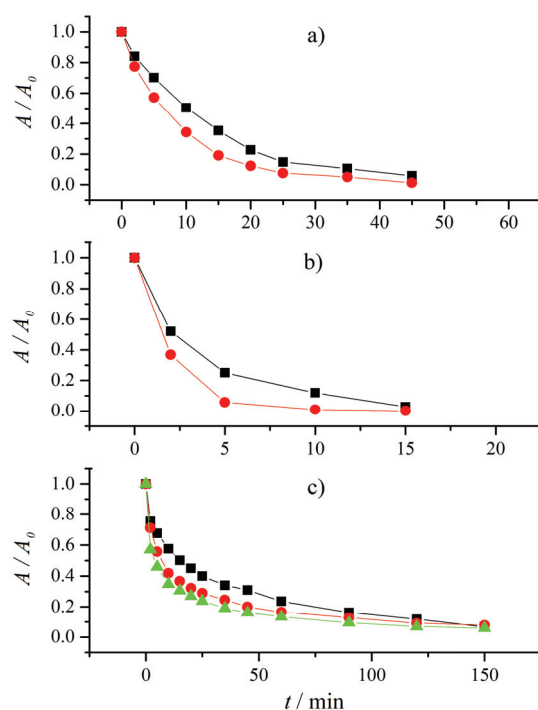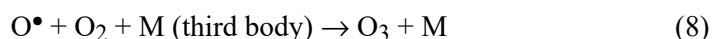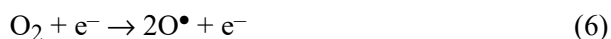

Fig. 6. Decolourisation rates of textile dyes: a) RO 16, b) RB 19 and c) DR 28 during plasma treatment for different composition (-■- 2 % O_2, -●- 5 % O_2, -▲- 10 % O_2) of feed gas (4 dm^3 min^{-1}).

Namely, the time for the total oxidation was shortened from 60 to 15 min (2 %) and even faster decolourisation was accomplished (5 min) by increasing the O_2 amount (5 %) in the feed gas. The similar trend is observed for RO 16. The required time for total decolourisation outcome was reduced from 60 to 45 min but the difference between 2 and 5 % of O_2 did not influence the decolourisation rate degree as for RB 19. Fig. 6 also reveals the fact that the DR 28 was again the most problematic to decolourise even with the O_2 included (2 and 5 %). The time for the final oxidation result was evidently shorter, but still very

long, and the increase of the O_2 amount in the feed gas was proposed to 10 %. However, the satisfactory results were not attained because the treatment time was still very long (150 min).

According to the Gumuchian *et al*., the better oxidation rates of all dyes can be attributed to the higher concentration of excited hydroxyl radicals in the mixture of Ar and O_2 as feed gas than for pure Ar.[35] Besides this, with introducing the O_2 in the feed gas the generation of O and O_3 as the leading oxygen-based active species is enlarged. When O_2 is in contact to an electrical discharge, O atom (E^0 = 2.42 V) could be generated *via* dissociation of O_2 (Eq. (6)) and directly react with contaminants or it could improve $^{\bullet}$OH production (Eq. 7):[35–37]

$$O_2 + e^- \rightarrow 2O^{\bullet} + e^- \tag{6}$$

$$O^{\bullet} + H_2O \rightarrow 2^{\bullet}OH \tag{7}$$

$$O^{\bullet} + O_2 + M \text{ (third body)} \rightarrow O_3 + M \tag{8}$$

Additionally, O atom could also participate in reactions with O_2 resulting in the formation of O_3 (E^0 = 2.07 V), which has a relatively long half-life of about 15 min (Eq. (8)) and rapidly destructs the conjugated chains of the dye molecules (responsible for the colour intensity) leading to fast oxidation with rate constants in the range of 10^3 and 10^7 L mol^{-1} s^{-1}).[10]

Therefore, various active species are generated under different operating conditions, which could explain the difference between the decolourization rates for all dyes. In the case with pure Ar, $^{\bullet}$OH is the dominant reactant[35] but with O_2 included, a large amount of oxygen-based species are formed leading to a better decolourisation efficiency. This is consistent with the results of Jiang *et al*. who previously demonstrated that the plasma oxidation treatment was the best with O_2 as the feed gas followed by air and Ar, and the least for nitrogen.[36]

GRNN development and results

The input layer of the GRNN used in this study consisted of 3 neurons (one for each input variable), the pattern layer had one neuron for each pattern (Table S-I of the Supplementary material to this paper), the summation layer was composed of two neurons (one for the only output variable plus one), and the output layer had one neuron for the output variable (Fig. 3). After the architecture parameters were set, the GRNN was trained using the genetic adaptive module provided by Neuroshell2.[38] It uses a genetic algorithm to find the optimal values of the individual smoothing factors (ISFs) for each input as well as an overall smoothing factor (SF). The SF determines the GRNN accuracy, while the ISFs can be used for sensitivity analysis since their values indicate the significance of the input, *i.e.*, the input with larger ISF value is more important to the model.[39]

Available data for each dye was randomly split into three datasets, namely a training dataset for weights adjustment, a validation dataset for smoothing factor determination, and a test dataset for assessment the GRNN generalization performance, in the ratio 65–70:20:10–15, respectively, depending on the initial size of the available data. Descriptive statistics for each dataset are presented in Table S-II,a–c (Supplementary material). The performance of each GRNN model is described by common performance metrics in Fig. 7 and Table S-I.
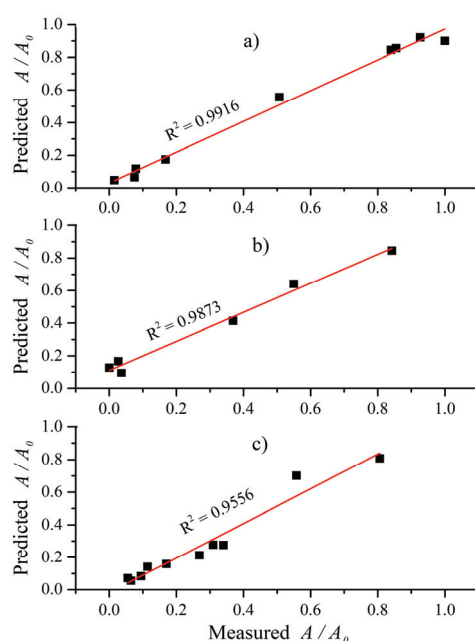

Fig. 7. Measured and predicted absorbances (by GRNN) of the decolourisation process for the textile dyes: a) RO 16, b) RB 19 and c) DR 28.

The low values of *RMSE* and *MAE*, as well as the high values of R^2 ($R^2 >$ 0.95), indicated that the data was very well fitted by the GRNN models. Furthermore, sensitivity analysis performed using the obtained *ISF* values (Table II) confirms that the significance of each input was well captured by the created models. Namely, Table II also reveals that the most dominant factor for the plasma decolourisation process of RO 16 and DR 28 generally was the treatment time.

TABLE II. Evaluation of the GRNN sensitivity analysis based on the *ISF* values for inputs used in the created models

Name	RO 16	RB 19	DR 28
t / min	2.64	2.11	2.76
Q / dm^3 min^{-1}	0.74	2.25	1.56
O$_2$ content, %	0.66	0.91	0.13

The significance of flow rate and composition of the feed gas were dependent on the specific dye. In the case of RO 16, the flow rate and amount of O_2 contributed to the effectiveness of the oxidation almost equally, unlike for DR 28 where the amount of O_2 was the least important. The influence of O_2 was the most perceptible for RB 19 treatment, when the decolourisation was much faster than in pure Ar for the same flow rate. Still, two crucial parameters (of the same importance) for the RB 19 oxidation process were the treatment time and Ar flow rate.

CONCLUSIONS

In this article, the plasma needle was presented as an effective technology for decolourisation of the various organic dyes (RO 16, RB 19 and DR 28). The decolourisation effects were correlated to the different molecular structures of the tested azo and anthraquinone dyes, duration of the treatment, and quality and quantity of the feed gas. It was established that the treatment time, Ar flow rate and O_2 content in the feed gas had different effects on the decolourisation rate for each colour. The increase of the Ar flow rate and O_2 content generally improved the oxidation rate but depending on the dye molecule, it was more or less noticeable. Due to its molecular structure, the azo dye DR 28 exhibited the smallest decolourisation rate compared to RO 16 and RB 19, even with increases in the Ar flow rate and O_2 content. RB 19 was easier to decolourise than DR 28, but the introduction of O_2 in the feed gas remarkably influenced its oxidation degree, reducing the time for total colour loss from 90 to 15 min (5 % O_2). The dye RO 16 achieved the highest oxidation rate and changing feed gas conditions led to even better oxidation performances.

According to the ANN models, the decolourisation efficiency could be predicted with satisfactory accuracy ($R^2 > 0.95$). These models also suggest that the duration of the plasma oxidation process was the most influential factor for the decolourisation effectiveness for RO 16 and DR 28. However, the feed gas flow rate and composition were very significant for RB 19 oxidation, unlike RO 16 where both parameters had the same (smaller) effect on the oxidation result. The Ar flow rate manifested a higher contribution degree to the DR 28 oxidation process than the amount of O_2 in the feed gas. Furthermore, the oxidation of DR 28 was optimized by investigations of the simultaneous application of a heterogeneous semiconductor photocatalyst together with the plasma. It is also planned to identify RO 16, RB 19 and DR 28 oxidation by-products and determine their toxicity level. Future work is planned in enhancing the present methodology by using the design of experiments, which will contribute to obtaining a dataset more suitable for multidimensional interpolation.

SUPPLEMENTARY MATERIAL

Additional data are available electronically from http://www.shd.org.rs/JSCS/, or from the corresponding author on request.

И З В О Д

ANN ПРЕДИКЦИЈА ЕФИКАСНОСТИ ДЕКОЛОРИЗАЦИЈЕ ОРГАНСКИХ БОЈА У ОТПАДНОЈ ВОДИ ПЛАЗМА ИГЛОМ

ТАТЈАНА Ђ. МИТРОВИЋ[1], МИРЈАНА Ђ. РИСТИЋ[2], АЛЕКСАНДРА ПЕРИЋ-ГРУЈИЋ[2] и САША ЛАЗОВИЋ[3]

[1]*Инсшишуш за водопривреду „Јарослав Черни", Беоīрад,* [2]*Универзишеш у Беоīраду, Технолошко–меша-лурīки факулшеш, Беоīрад и* [3]*Универзишеш у Беоīраду, Инсшишуш за физику, Беоīрад*

У овом раду представљени су резултати деколоризације текстилних боја RO 16, RB 19 и DR 28 у воденом раствору. Време третмана, проток носећег гаса (1, 4 и 8 $dm^3 min^{-1}$) и састав гаса (Ar, Ar/O_2) су мењани у циљу проналажења оптималних параметара за најбоље перформансе третмана плазмом за сваку боју. Вештачке неуронске мреже (ANN) су коришћене за предвиђање параметара који имају кључну улогу у процесу деколоризације. Постигнуто је 95 % деколоризације за све три боје након третмана плазмом. Деколоризација DR 28 је била много спорија од друге две боје због сложености његове молекуларне структуре. Закључено је да оксидација зависи од сва три наведена параметра. Модел је предвидио време третмана као најдоминантнији фактор за најбоље резултате деколоризације RO 16 и DR 28 и протока за Ar RB 19. Потврдили смо да је плазма игла врло корисна метеода за оксидацију органских загађујућих материја и да се АНН може користити за предвиђање параметара у циљу побољшања ефикасности третмана плазмом.

(Примљено 4. октобра, ревидирано 25. децембра, прихваћено 30. децембра 2019)

REFERENCES

1. E. Bizani, K. Fytianos, I. Poulios, V. Tsiridis, *J. Hazard. Mater.* **136** (2006) 85 (http://dx.doi.org/10.1016/j.jhazmat.2005.11.017)
2. S. Dutta, R. Saha, H. Kalita, A. Bezbaruah, *Environ. Technol. Innov.* **5** (2016) 176 (http://dx.doi.org/10.1016/j.eti.2016.03.001)
3. E. Basturk, M. Karatas, *Ultrason. Sonochem.* **21** (2014) 1881 (http://dx.doi.org/10.1016/j.ultsonch.2014.03.026)
4. J. Gao, Q. Zhang, K. Su, R. Chen, Y. Peng, *J. Hazard. Mater.* **174** (2010) 215 (http://dx.doi.org/10.1016/j.jhazmat.2009.09.039)
5. B. Dojcinovic, *PhD Thesis*, Faculty of Chemistry, Belgrade, 2011
6. Z. Cheng, L. Zhang, X. Guo, X. Jiang, T. Li, *Spectrochim. Acta, A.* **137C** (2014) 1126 (http://dx.doi.org/10.1016/j.saa.2014.08.138)
7. H. Ali, *Water*, *Air Soil Pollut.* **213** (2010) 251 (http://dx.doi.org/10.1007/s11270-010-0382-4)
8. A. R. Nešić, S. J. Veličković, D. G. Antonović, *Compos., B* **53** (2013) 145 (http://dx.doi.org/10.1016/j.compositesb.2013.04.053)
9. N. H. H. Hairom, A. W. Mohammad, A. A. H. Kadhum, *J. Water Process Eng.* **4** (2014) 99 (http://dx.doi.org/10.1016/j.jwpe.2014.09.008)
10. C. Tizaoui, N. Grima, *Chem. Eng. J.* **173** (2011) 463 (http://dx.doi.org/10.1016/j.cej.2011.08.014)

11. V. Janaki, K. Vijayaraghavan, A. K. Ramasamy, K. Lee, B. T Oh, S. Kamala-Kannan, *J. Hazard. Mater.* **241**–**242** (2012) 110 (http://dx.doi.org/10.1016/j.jhazmat.2012.09.019)

12. Y. Sun, Y. Liu, R. Li, G. Xue, S. Ognier, *Chemosphere* **155** (2016) 243 (http://dx.doi.org/10.1016/j.chemosphere.2016.04.026)

13. N. Haddou, M. R. Ghezzar, F. Abdelmalek, S. Ognier, M. Martel, A. Addou, *Chemosphere* **107** (2014) 304 (http://dx.doi.org/10.1016/j.chemosphere.2013.12.071)

14. B. P. Dojčinović, B. M. Obradović, M. M. Kuraica, M. V. Pergal, S. D. Dolić, D. R. Indić, T. B. Tosti, D. D. Manojlović, *J. Serb. Chem. Soc.* **81** (2016) 829 (http://dx.doi.org/10.2298/JSC160105030D)

15. M. Hijosa-Valsero, R. Molina, H. Schikora, M. Müller, J. M. Bayona, *J. Hazard. Mater.* **262** (2013) 664 (http://dx.doi.org/10.1016/j.jhazmat.2013.09.022)

16. M. Tichonovas, E. Krugly, V. Racys, R. Hippler, V. Kauneliene, I. Stasiulaitiene, D. Martuzevicius, *Chem. Eng. J.* **229** (2013) 9 (http://dx.doi.org/10.1016/j.cej.2013.05.095)

17. Y. Sun, R. Li, G. Xue, S. Ognier, *Chemosphere* **155** (2016) 243 (https://doi.org/10.1016/j.chemosphere.2016.04.026)

18. T. Wang, G. Qu, J. Ren, Q. Sun, D. Liang, S. Hu, *J. Hazard. Mater.* **302** (2016) 65 (http://dx.doi.org/10.1016/j.jhazmat.2015.09.051)

19. N. Puač, D. Maletić, S. Lazović, G. Malović, A. Orević, Z. L. Petrović, N. Puač, D. Maletić, S. Lazović, G. Malović, A. Dordević, Z. L. J. Petrović, *Appl. Phys. Lett.* **101** (2012) 2010 (http://dx.doi.org/10.1063/1.4735156)

20. R. P. Joshi, S. M. Thagard, *Plasma Chem. Plasma Process.* **33** (2013) 17 (http://dx.doi.org/10.1007/s11090-013-9436-x)

21. P. Lukes, E. Dolezalova, I. Sisrova, M. Clupek, *Plasma Sources Sci. Technol.* **23** (2014) 015019 (http://dx.doi.org/10.1088/0963-0252/23/1/015019)

22. A. Cabrera Reina, L. Santos-Juanes Jordá, J. L. García Sánchez, J. L. Casas López, J. A. Sánchez Pérez, *Appl. Catal., B* **119**–**120** (2012) 132 (http://dx.doi.org/10.1016/j.apcatb.2012.02.021)

23. R. Zaplotnik, M. Bišćan, Z. Kregar, U. Cvelbar, M. Mozetič, S. Milošević, *Spectrochim. Acta,B* **103**–**104** (2015) 124 (http://dx.doi.org/10.1016/j.sab.2014.12.004)

24. S. Heddam, H. Lamda, S. Filali, *Environ. Process.* **3** (2016) 153 (http://dx.doi.org/10.1007/s40710-016-0129-3)

25. K. Munro, T. H. Miller, C. P. B. Martins, A. M. Edge, D. A. Cowan, L. P. Barron, *J. Chromatogr., A* **1396** (2015) 34 (http://dx.doi.org/10.1016/j.chroma.2015.03.063).

26. H. Simsek, *Environ. Technol. (UK)* **37** (2016) 2879 (http://dx.doi.org/10.1080/09593330.2016.1167964)

27. X. Zhang, Y. Zhu, X. Chen, W. Shen, R. Lute, *J. Bioresour. Bioprod.* **3** (2018) 71 (http://dx.doi.org/10.21967/jbb.v3i2.112)

28. D. F. Specht, *IEEE Trans. Neural Networks* **2** (1991) 568 (http://dx.doi.org/10.1109/72.97934)

29. M. D. Radović, J. Z. Mitrović, D. V. Bojić, M. D. Antonijević, M. M. Kostić, R. M. Baošić, A. L. Bojić, *Water SA* **40** (2014) 571 (http://dx.doi.org/10.4314/wsa.v40i3.21).

30. M. A. N. Khan, M. Siddique, F. Wahid, R. Khan, *Ultrason. Sonochem.* **26** (2015) 370 (http://dx.doi.org/10.1016/j.ultsonch.2015.04.012)

31. S. Bilgi, C. Demir, *Dyes Pigments* **66** (2005) 69 (http://dx.doi.org/10.1016/j.dyepig.2004.08.007)

32. C. Guillard, H. Lachheb, A. Houas, M. Ksibi, E. Elaloui, J.-M. M. Herrmann, *J. Photochem. Photobiol., A* **158** (2003) 27 (http://dx.doi.org/10.1016/S1010-6030(03)00016-9)

33. U. Isah A., G. Abdulraheem, S. Bala, S. Muhammad, M. Abdullahi, *Int. Biodeterior. Biodegradation* **102** (2015) 265 (http://dx.doi.org/10.1016/j.ibiod.2015.04.006)
34. K. K. Panda, A. P. Mathews, *Chem. Eng. J.* **255** (2014) 553 (http://dx.doi.org/10.1016/j.cej.2014.06.071)
35. D. Gumuchian, S. Cavadias, X. Duten, M. Tatoulian, P. Da Costa, S. Ognier, *Chem. Eng. Process. Process Intensif.* **82** (2014) 185 (http://dx.doi.org/10.1016/j.cep.2014.06.003).
36. B. Jiang, J. Zheng, S. Qiu, M. Wu, Q. Zhang, Z. Yan, Q. Xue, *Chem. Eng. J.* **236** (2014) 348 (http://dx.doi.org/10.1016/j.cej.2013.09.090)
37. Y. Miyazaki, K. Satoh, H. Itoh, *Electr. Eng. Japan* **174** (2011) 1 (http://dx.doi.org/10.1002/eej.20937)
38. Ward Systems Group Inc. NeuroShell 2 (2008) Available at: http://www.wardsystems.com (Accesses: 22nd July 2019)
39. D. Z. Antanasijević, M. D. Ristić, A. A. Perić-Grujić, V. V. Pocajt, *Int. J. Greenh. Gas Control* **20** (2014) 244 (http://dx.doi.org/10.1016/j.ijggc.2013.11.011).